

Imidazopyridine/Pyrrole and Hydroxybenzimidazole/Pyrrole Pairs for DNA Minor Groove Recognition

Dorte Renneberg and Peter B. Dervan*

Contribution from the Division of Chemistry and Chemical Engineering, California Institute of Technology, Pasadena, California 91125

Received January 7, 2003; E-mail: dervan@caltech.edu.

Abstract: The DNA binding properties of fused heterocycles imidazo[4,5-*b*]pyridine (**Ip**) and hydroxybenzimidazole (**Hz**) paired with pyrrole (**Py**) in eight-ring hairpin polyamides are reported. The recognition profile of **Ip/Py** and **Hz/Py** pairs were compared to the five-membered ring pairs **Im/Py** and **Hp/Py** on a DNA restriction fragment at four 6-base pair recognition sites which vary at a single position 5'-TGTNTA-3', where N = G, C, T, A. The **Ip/Py** pair distinguishes G•C from C•G, T•A, and A•T, and the **Hz/Py** pair distinguishes T•A from A•T, G•C, and C•G, affording a new set of heterocycle pairs to target the four Watson–Crick base pairs in the minor groove of DNA.

Introduction

Many diseases are related to aberrant gene expression and the ability to reprogram transcription in a cell by chemical methods could be important in biology and human medicine.¹ Minor-groove-binding polyamides which bind predetermined DNA sequences offers one approach to artificial gene regulation.² These molecules are based on analogues of the pyrrole ring **Py** of the natural products netropsin and distamycin A which bind in the minor groove of DNA.³ Base-pair specificity can be altered by changing the functional group(s) presented to the floor of the DNA minor groove.⁴ Stabilizing and destabilizing interactions with the different edges of the four Watson–Crick base pairs are modulated by specific hydrogen-bonds and shape complementarity. For example, the imidazole residue **Im** presents the DNA with the N-atom and its lone pair electrons which can accept a H-bond from the exocyclic NH₂ of G. Additionally, the 3-hydroxypyrrole residue **Hp** presents an OH group that is sterically accommodated opposite T not A and, in addition, can donate H-bonds to the O(2) of thymine. For discrimination of each of the Watson–Crick base pairs, unsym-

metrical pairs of five-membered rings appear to be the best solution such that **Im/Py** is specific for G•C and **Hp/Py** for T•A.⁴

The pairing rules have proven useful for the recognition of hundreds of DNA sequences by polyamides. However, sequence-dependent DNA structural variation makes binding affinity and specificity at many DNA sequences unpredictable, which leads us to continue our search for new heterocycles of slightly different shape, curvature and twist for minor-groove recognition.^{5–7} Importantly, we find that polyamides containing **Hp** residues can degrade over time in the presence of acid or free radicals, and a robust replacement for use in biological studies is desirable. Several five-membered heterocyclic residues other than **Py**, **Im**, and **Hp** have been investigated, including furan **Fr**, thiazole **Nt**, pyrazole **Pz**, and 3-hydroxythiophene **Ht** with no new specificity uncovered.^{6d} In retrospect, it is remarkable that a search of new five-membered heterocycles (and new heterocycle pairs) reveals few new leads for sequence discrimination. This implies that the solution to DNA recognition by **Im/Py**, **Py/Im**, **Hp/Py**, and **Py/Hp** could be a narrow structural window. We attempt to broaden the repertoire of aromatic heterocycles for DNA recognition by exploring a family of benzimidazoles with different atomic substitutions (CH, N, OH) on the *six-membered* ring directed toward the floor of the DNA minor groove. Curvature effects are amplified in contiguous-ring polyamides where π -conjugation limits conformational flexibility. The pyrrole ring appears slightly over-curved with

- (1) (a) Darnell, J. E. *Nature Rev.* **2002**, 2, 740–748. (b) Pandolfi, P. P. *Oncogene* **2001**, 20, 3116–3127.
(2) (a) Gottesfeld, J. M.; Neely, L.; Trauger, J. W.; Baird, E. E.; Dervan, P. B. *Nature* **1997**, 387, 202–205. (b) Dickinson, L. A.; Gulizia, R. J.; Trauger, J. W.; Baird, E. E.; Mosier, D. E.; Gottesfeld, J. M.; Dervan, P. B. *Proc. Natl. Acad. Sci. U.S.A.* **1998**, 95, 12 890–12 895. (c) Janssen, S.; Durussel, T.; Laemmli, U. K. *Mol. Cell.* **2000**, 6, 999–1011. (d) Ansari, A. Z.; Mapp, A. K.; Nguyen, D. H.; Dervan, P. B.; Ptashne, M. *Chem. Biol.* **2001**, 8, 583–592. (e) Coull, J. J.; He, G.; Melander, C.; Rucker, V. C.; Dervan, P. B.; Margolis, D. M. *J. Virology* **2002**, 76, 12 349–12 354.
(3) (a) Dervan, P. B.; Bürl, R. W. *Curr. Opin. Chem. Biol.* **1999**, 3, 688–693. (b) Wemmer, D. E. *Biopolymers* **1999**, 52, 197–211. (c) Dervan, P. B. *Bioorg. Med. Chem.* **2001**, 9, 2215–2235.
(4) (a) White, S.; Szewczyk, J. W.; Turner, J. M.; Baird, E. E.; Dervan, P. B. *Nature* **1998**, 391, 468–471. (b) Kielkopf, C. L.; White, S.; Szewczyk, J. W.; Turner, J. M.; Baird, E. E.; Dervan, P. B.; Rees, D. C. *Science* **1998**, 282, 111–115. (c) Kielkopf, C. L.; Bremer, R. E.; White, S.; Szewczyk, J. W.; Turner, J. M.; Baird, E. E.; Dervan, P. B.; Rees, D. C. *J. Mol. Biol.* **2000**, 295, 557–567.

- (5) Ellervik, U.; Wang, C. C. C.; Dervan, P. B. *J. Am. Chem. Soc.* **2000**, 122, 9354–9360.
(6) (a) Zhan, Z. Y. J.; Dervan, P. B. *Bioorg. Med. Chem.* **2000**, 8, 2467–2474. (b) Nguyen, D. H.; Szewczyk, J. W.; Baird, E. E.; Dervan, P. B. *Bioorg. Med. Chem.* **2001**, 9, 7–17. (c) O'Hare, C. C.; Mack, D.; Tandon, M.; Sharma, S. K.; Lown, J. W.; Kopka, M. L.; Dickerson, R. E.; Hartley, J. A. *Proc. Natl. Acad. Sci. U.S.A.* **2002**, 99, 72–77. (d) Marques, M. A.; Doss, R. M.; Urbach, A. R.; Dervan, P. B. *Helv. Chim. Acta* **2002**, in press.
(7) Kielkopf, C. L.; Baird, E. E.; Dervan, P. B.; Rees, D. C. *Nature Struct. Biol.* **1998**, 5, 104–109.

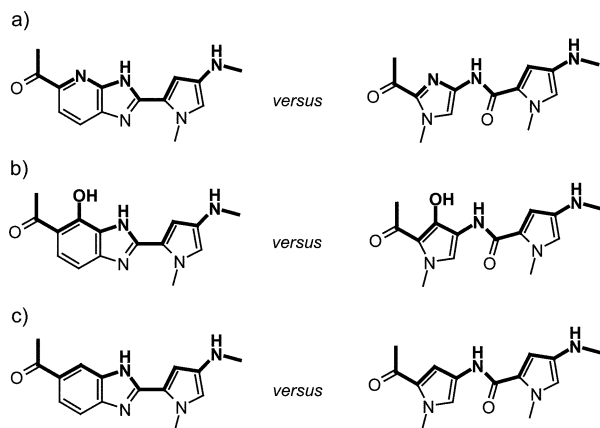


Figure 1. Structures of the (a) imidazo[4,5-*b*]pyridine, (b) hydroxybenzimidazole, and (c) benzimidazole building blocks in comparison with their respective five-membered ring systems. H-bonding surfaces along the recognition sites are highlighted.

respect to the DNA helix, likely leading to less optimal contact.⁷ We would anticipate that polyamides with benzimidazole substitutions would have a smaller degree of curvature compared with the five-membered rings^{8–11} which might improve the polyamide–DNA minor groove fit. Recently, we found that the incorporation of a benzimidazole (**Bi**) into an eight-ring hairpin polyamide leads to minor groove binding ligands with no loss in affinity when paired opposite a five-membered ring **Im** and that the **Im/Bi** pair specifies for G•C similar to the **Im/Py** pair.¹¹

We report here the synthesis of two benzimidazole analogues, imidazo[4,5-*b*]pyridine (**Ip**), hydroxybenzimidazole (**H**z) amino acids and their incorporation into eight-ring hairpin polyamides by solid-phase methods.¹² Their DNA binding affinities and relative sequence specificities were analyzed by quantitative DNase I footprint titration on a DNA restriction fragment and compared to the well-characterized **Im**, **Hp** and **Py** hairpin

polyamides. In a formal sense, analogues of benzimidazole–pyrrole keep the same atomic connectivity along the inside recognition edge as their parent five-membered ring systems (Figure 1). It is anticipated that the NH proton N(3)–H of the fused imidazole unit can form H-bonds with lone pairs of N(3) of purines and O(2) of pyrimidines. The key unknown issue is whether the pyridine nitrogen on the inside edge of the imidazo[4,5-*b*]pyridine building block is capable of forming a sequence-specific H-bond to the exocyclic NH₂ of G. Specifically, does the **Ip/Py** pair mimic an **Im/Py** pair by distinguishing G•C from C•G? In the case of the hydroxybenzimidazole **H**z, the question arises whether the hydroxyl group on the inside edge of the ligand can form a H-bond with the O(2) of thymine. Does the **H**z/**Py** pair mimic **Hp/Py** and distinguish T•A from A•T? A schematic drawing of the polyamide–DNA complexes including the postulated hydrogen bonds is illustrated in Figure 2.

For the present study, six eight-ring polyamides, **ImPyIpPy**-(*R*)^{H2N}-PyPyPyPy-CONHMe (**1**), **ImPyH**zPy-(*R*)^{H2N}-PyPyPyPy-CONHMe (**2**), and **ImPyBiPy**-(*R*)^{H2N}-PyPyPyPy-CONHMe (**3**) as well as the corresponding all five-membered ring hairpins **ImPyImPy**-(*R*)^{H2N}-PyPyPyPy-CONHMe (**4**), **ImPyHpPy**-(*R*)^{H2N}-PyPyPyPy-CONHMe (**5**), and **ImPyPyPy**-(*R*)^{H2N}-PyPyPyPy-CONHMe (**6**) were synthesized (Figure 3). The plasmid pDR1 was designed containing four 6-base pair binding sites 5'-TGTNTA-3' (N = G, C, T, A) which differ by a single internal binding position allowing us to determine their match and single base pair mismatch DNA binding properties for the four Watson–Crick base pairs in the minor groove of DNA (Figure 4).

Results and Discussion

Monomer Syntheses. For the synthesis of the *N*-Boc-protected imidazo[4,5-*b*]pyridine–pyrrole building block (Boc-PyIp-OH, **15**) we chose the commercially available 2,6-dichloro-

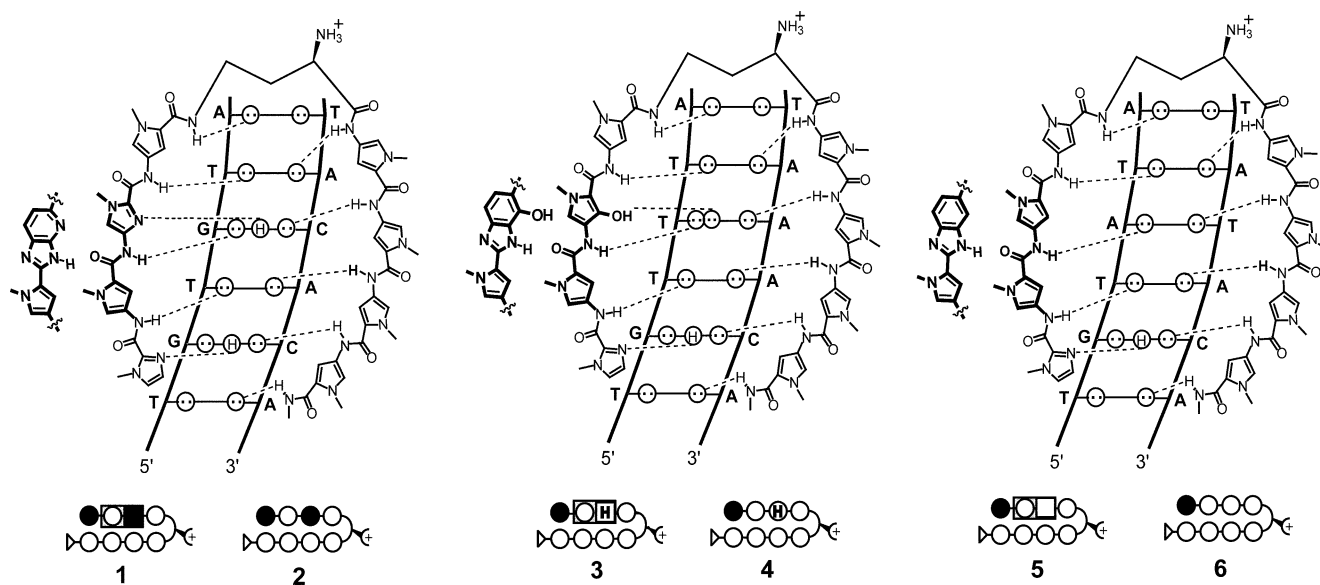


Figure 2. Postulated hydrogen-bonding models of the 1:1 polyamide–DNA complexes formed between the imidazo[4,5-*b*]pyridine-containing polyamide **ImPyIpPy**-(*R*)^{H2N}-PyPyPyPy-CONHMe (**1**), the hydroxybenzimidazole-containing polyamide **ImPyH**zPy-(*R*)^{H2N}-PyPyPyPy-CONHMe (**2**), the benzimidazole-containing polyamide **ImPyBiPy**-(*R*)^{H2N}-PyPyPyPy-CONHMe (**3**) as well as their parent five-membered ring-containing polyamides **ImPyImPy**-(*R*)^{H2N}-PyPyPyPy-CONHMe (**4**), **ImPyHpPy**-(*R*)^{H2N}-PyPyPyPy-CONHMe (**5**), and **ImPyPyPy**-(*R*)^{H2N}-PyPyPyPy-CONHMe (**6**) and their respective match sequences 5'-TGTGTA-3' (for **1** and **2**), 5'-TGTTTA-3' (for **3** and **4**), and 5'-TGTATA-3' (for **5** and **6**), respectively. Circles with two dots represent the lone pairs of N(3) of purines and O(2) of pyrimidines. Circles containing an "H" represent the N(2) hydrogen of G. Putative hydrogen bonds are illustrated by dotted lines. The incorporated imidazo[4,5-*b*]pyridine–imidazole–pyrrole, hydroxybenzimidazole–hydroxypyrrrole–pyrrole, and benzimidazole–pyrrole–pyrrole moieties are shown in bold. Below each hydrogen-bonding model are the ball-and-stick representations of the polyamides.

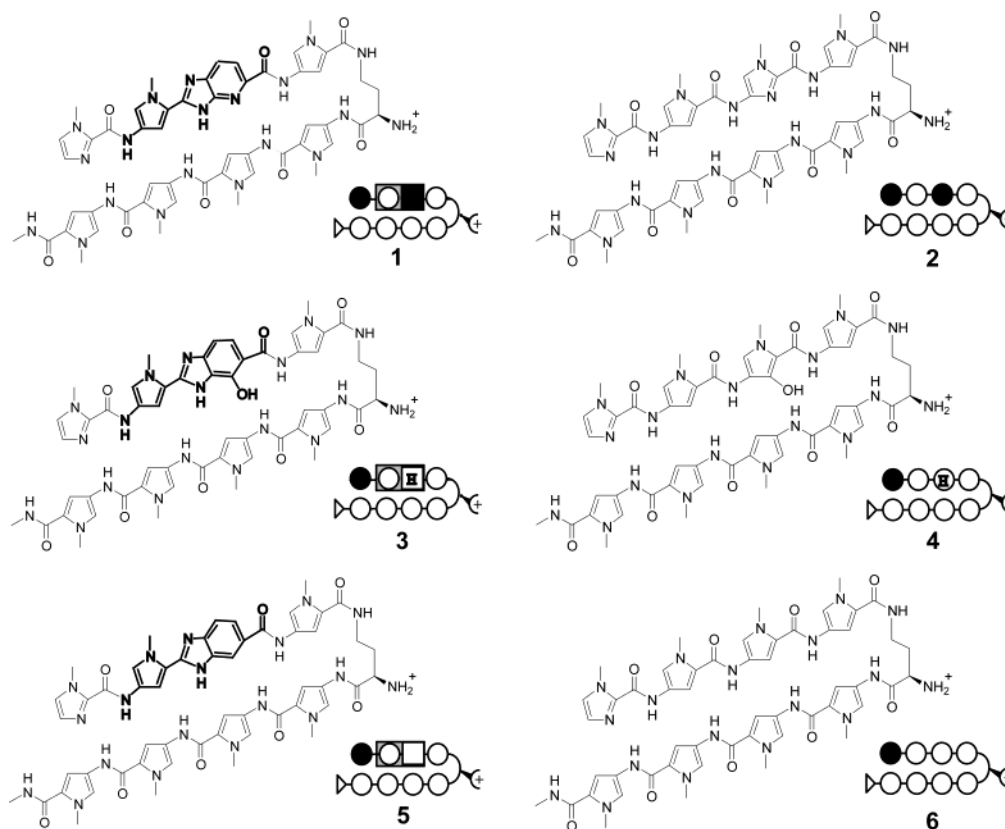


Figure 3. Structures of the six-membered-ring fused heterocycles containing eight-ring polyamides **1**, **3**, and **5**, and the corresponding parent polyamides **2**, **4**, and **6**. Ball-and-stick models are shown with shaded and nonshaded circles indicating imidazole and pyrrole carboxamides, respectively, whereas hydroxypyrrole rings are annotated with an "H" in the center of an unshaded sphere. Two touching squares represent the six-membered ring systems attached to a pyrrole: the shaded square represents the imidazo[4,5-*b*] unit, the nonshaded square with an "H" in the center the hydroxybenzimidazole unit, and the nonshaded square represents the benzimidazole unit, the adjacent pyrrole is depicted as a nonshaded circle inside the second square as described above. (*R*)-Diaminobutyric acid (DAB) (**a**) is depicted as a curved line and a plus sign, the methyl amide tail is annotated as a triangle.



Figure 4. Illustration and complete sequences of the *EcoRI*/*PvuII* restriction fragment derived from plasmid pDR1. The four designed 6-base pair binding sites that were analyzed in quantitative footprint titrations are shown in bold and surrounded by a box.

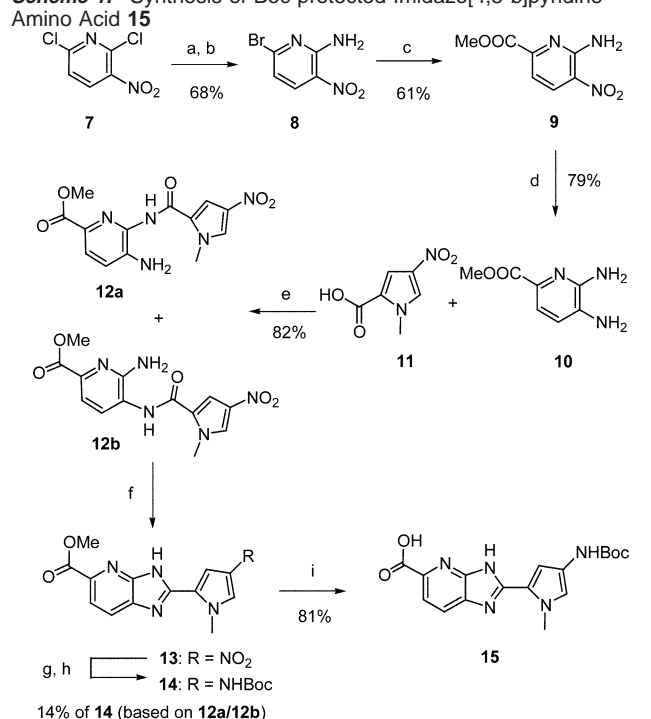
3-nitropyridine (**7**) as starting material (Scheme 1). Nitropyridine **7** was converted to 6-bromo-3-nitropyridin-2-ylamine (**8**) via halogen exchange¹³ in both *ortho*-positions with HBr in acetic acid followed by treatment with NH₃/MeOH to regioselectively substitute one of the two bromo substituents.¹⁴ The introduction of the methyl ester functionality was then accomplished via a palladium-catalyzed carbonylation.^{15,16} In the presence of carbon monoxide, MeOH, Et₃N, and catalytic amounts of Pd(OAc)₂ and PPh₃, the conversion of **8** proceeded smoothly and methyl ester **9** could be isolated in 61% yield. Systematic variation of the reaction conditions, e.g., CO pressure, temperature and

catalytic system (PdCl₂(PPh₃)₃; Pd(OAc)₂, Dppp) did not show any effect on reaction time or yield. Reduction of the nitro group in **9** with Pd/C in the presence of hydrogen gave the corresponding *ortho*-diamine **10** in 63% yield.

The key step for the synthesis of the imidazo[4,5-*b*]pyridine-pyrrole unit is a cyclocondensation. The first step, a HBTU mediated coupling of diamine **10** with carboxylic acid **11** resulted in a mixture of the two isomeric amino amides **12a** and **12b** which were then transformed to the desired imidazo[4,5-*b*]pyridine **13** by heating at 80–90 °C in glacial acetic acid. Note that similar cyclocondensation steps of amino amides usually require higher temperatures of 120–140 °C.¹⁷ However, compounds **12a** and **12b** were unstable under these conditions, and no cyclization product could be isolated. Due to purification

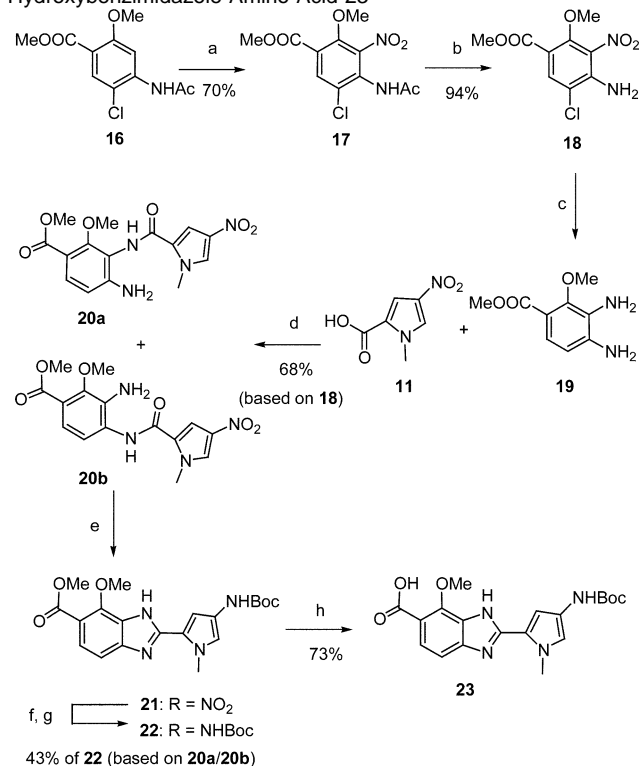
- (8) (a) Minehan, T. G.; Gottwald, K.; Dervan, P. B. *Helv. Chim. Acta* **2000**, *83*, 2197–2213. (b) Ji, Y.-H.; Bur, D.; Haesler, W.; Schmitt, V. R.; Dorn, A.; Bailly, C.; Waring, M. J.; Hochstrasser, R.; Leupin, W. *Bioorg. Med. Chem.* **2001**, *9*, 2905–2919. (c) Singh, M. P.; Joseph, T.; Kumar, S.; Bathini, Y.; Lown, J. W. *Chem. Res. Toxicol.* **1992**, *5*, 579–607.
- (9) Singh, A. K.; Lown, J. W. *Anti-Cancer Drug Design* **2000**, *15*, 265–275.
- (10) Bathini, Y.; Rao, K. E.; Shea, R. G.; Lown, J. W. *Chem. Res. Toxicol.* **1990**, *3*, 268–280.
- (11) Briehn, C. A.; Weyermann, P.; Dervan, P. B. *Eur. J. Chem.*, in press.

- (12) (a) Baird, E. E.; Dervan, P. B. *J. Am. Chem. Soc.* **1996**, *118*, 6141–6146. (b) Belitsky, J. M.; Nguyen, D. H.; Wurtz, N. R.; Dervan, P. B. *Bioorg. Med. Chem.* **2002**, *10*, 2767–2774.
- (13) Mutterer, F.; Weis, C. D. *Helv. Chim. Acta* **1976**, *59*, 229–235.
- (14) EP0995 742 AI

Scheme 1. Synthesis of Boc-protected Imidazo[4,5-*b*]pyridine

problems with **13** we decided to use the crude product directly in the next step. Thus, after evaporation of the glacial acetic acid, reduction of the nitro group in **13** with tin(II)chloride in DMF and in situ Boc protection yielded in the aromatic amino acid ester **14**. Final saponification of methyl ester **14** with sodium hydroxide in dioxane/H₂O afforded the desired *N*-Boc-protected imidazo[4,5-*b*]pyridine-pyrrole amino acid (Boc-PyIp-OH, **15**) in 81% yield.

For the synthesis of the *N*-Boc *O*-methyl-protected hydroxybenzimidazole-pyrrole building block (Boc-PyOz-OH, **23**) we also envisioned a cyclocondensation of the corresponding *ortho*-diamine and the carboxylic acid for the construction of the hydroxybenzimidazole unit. As starting material we chose 4-acetylaminobenzoic acid methyl ester (**16**), which is commercially available (Scheme 2). A regioselective nitration¹⁸ **17** followed by deacetylation of the amine under acidic conditions afforded methyl ester **18** in 66% yield over two steps, starting from **16**. Hydrogenation of **18** on 10% Pd/C in the presence of triethylamine in MeOH¹⁸ at r.t. afforded cleanly *ortho*-diamine **19**. The HBTU mediated coupling of diamine **19** and carboxylic acid **11** resulted in the two isomeric amino amides **20a** and **20b**, which cyclized by heating at 90 °C in glacial acetic acid **21**. Reduction of the nitro group in **21** with Pd/C in the presence of hydrogen, in situ Boc-protection of the free amine to obtain **22** and final hydrolysis of the methyl ester with sodium hydroxide in dioxane/H₂O gave the desired *N*-Boc-*O*-methyl-protected hydroxybenzimidazole-pyrrole (Boc-

Scheme 2. Synthesis of Boc-protected *O*-methyl Hydroxybenzimidazole Amino Acid **23**

PyOz-OH, **23**). The synthesis of the *N*-Boc-protected benzimidazole-pyrrole (Boc-PyBi-OH, **24**) will be reported elsewhere.¹¹

Polyamide Syntheses. The parent polyamides **2**, **6**, and the *O*-protected derivative of **4** (namely **32**) were synthesized following manual solid-phase methods¹² on Kaiser's oxime resin (0.48 mmol/g) in 17 steps. The building blocks employed for the stepwise oligomer elongation procedure were Boc-*N*-methyl pyrrole (Boc-Py-OBt, **25**), Boc-*N*-methyl imidazole (Boc-Im-OH, **26**), Boc-*N*-methyl methoxypyrrole (Boc-Op-OH, **27**) monomers, *N*-methyl imidazole (Im-OH, **28**) cap and α-Fmoc-γ-Boc-(*R*)-2,4-diaminobutyric acid (α-Fmoc-γ-Boc-(*R*)-DABA, **29**). For the synthesis of the imidazo[4,5-*b*]pyridine, hydroxybenzimidazole and benzimidazole containing polyamides **1**, **5**, and **31**, respectively, the same protocol could be applied successfully. Compounds **15**, **23**, and **24** were coupled in NMP/DIEA for 3 h at r.t. after activation with HBTU. Deprotection was achieved with 20% TFA/CH₂Cl₂. Following the general protocol summarized in Scheme 3, the synthesis of hairpin polyamides containing the fused heterocycles was carried out in 15 steps.

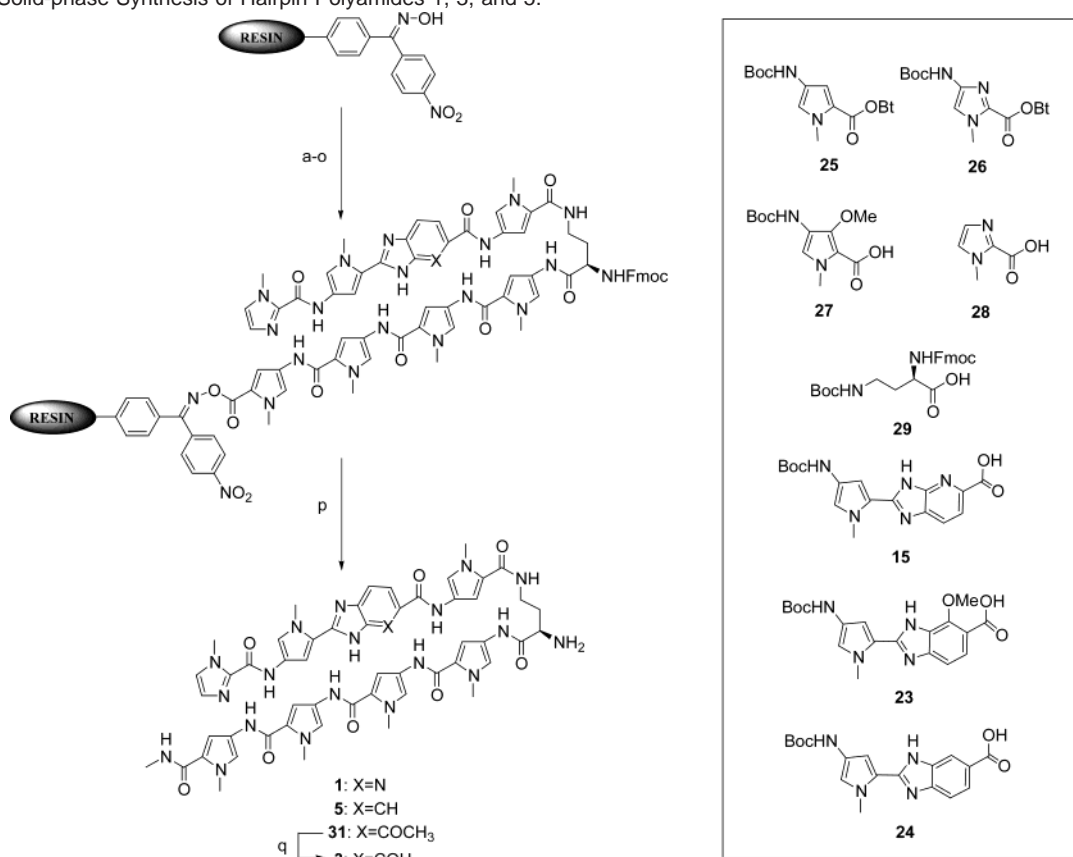
Cleavage from the resin and removal of the Fmoc group of the DABA turn was achieved by treatment with methylamine/CH₂Cl₂ (12 h, 37 °C). Following filtration of the resin, the crude mixtures were purified by reversed-phase HPLC to yield polyamides ImPyIpPy-(*R*)-H₂Nγ-PyPyPyPy-CONHMe (**1**), ImPyImPy-(*R*)-H₂Nγ-PyPyPyPy-CONHMe (**2**), ImPyOzPy-(*R*)-H₂Nγ-PyPyPyPy-CONHMe (**31**), ImPyOpPy-(*R*)-H₂Nγ-PyPyPyPy-CONHMe (**32**), ImPyBiPy-(*R*)-H₂Nγ-PyPyPyPy-CONHMe (**5**), and ImPyPyPy-(*R*)-H₂Nγ-PyPyPyPy-CONHMe (**6**). Subsequently, both *O*-methyl protected polyamides **31** and **32** were

(15) Schoenberg, A.; Bartoletti, I.; Heck, R. F. *J. Org. Chem.* **1974**, *39*, 3318–3326.

(16) Mägerlein, W.; Indolese, A. F.; Beller, M. *Angew. Chem., Int. Ed. Engl.* **2001**, *40*, 2856–2859.

(17) Wright, J. B. *Chem. Rev.* **1951**, *48*, 396–541.

(18) Tanaka, A.; Ito, K.; Nishino, S.; Motoyama, Y.; Takasugi, H. *Chem. Pharm. Bull.* **1994**, *42*, 560.

Scheme 3. Solid-phase Synthesis of Hairpin Polyamides 1, 3, and 5.

O-demethylated under identical conditions using ethanethiol/NaH protocol⁵ (80 °C, 30 min) and purified by reversed-phase HPLC to provide ImPyH_zPy-(*R*)^{H₂N}γ-PyPyPyPy-CONHMe (**3**) and ImPyHpPy-(*R*)^{H₂N}γ-PyPyPyPy-CONHMe (**4**).

Imidazo[4,5-*b*]pyridine/Pyrrole Pair. To examine whether an imidazo[4,5-*b*]pyridine unit **Ip** can replace a five-membered imidazole ring **Im** within an eight-ring hairpin polyamide regarding DNA binding affinity and specificity, polyamide **1** and its parent all five-membered ring hairpin **2** were evaluated by DNase I footprint titrations under identical conditions. Quantitative DNase I footprint titration experiments (10 mM Tris-HCl, 10 mM KCl, 10 mM MgCl₂, 5 mM CaCl₂, pH 7.0, 22 °C, equilibration time: 12 h)¹⁹ were performed on a ³²P-3'-labeled *Eco*RI/*Pvu*II restriction fragment of plasmid pDR1 0 (Figure 4). This DNA fragment contains four 6-base pair binding sites which differ at one position, 5'-TGTCTA-3', 5'-TGTTTA-3', 5'-TGTATA-3', and 5'-TGTGTA-3'. The latter one was regarded as the possible match site having a G•C base pair under the **Ip/Py** or **Im/Py** pair, respectively. Indeed, both polyamides **1** and **2** exhibit the same binding site preference (Figure 5). Parent **2** binds its match site 5'-TGTGTA-3' with an affinity of $K_a = 2.3 \times 10^9 \text{ M}^{-1}$ and shows a clear preference versus the C•G site by nearly a factor of 10. The affinities to A•T and T•A sites are lower, revealing modest specificity (4–8-fold). The imidazo[4,5-*b*]pyridine-containing polyamide **1**

binds the 5'-TGTGTA-3' site with an equilibrium association constant of $K_a = 1.2 \times 10^{10} \text{ M}^{-1}$, a 5-fold higher affinity than its parent compound **2** (Table 1. Although the A/T base pair mismatch recognition is similar, the introduction of the **Ip/Py** pair is accompanied with a slight decrease in binding specificity for the C•G base pair site. This encouraging result supports a model wherein the pyridine nitrogen of the imidazo[4,5-*b*]pyridine forms a specific H-bond to the exocyclic NH₂ of G.

Hydroxybenzimidazole/Pyrrole Pair. To examine whether the hydroxybenzimidazole unit **H_z** can replace a five-membered hydroxypyrrole ring **Hp**, polyamide **3** and its parent all five-membered ring hairpin **4** were compared. The all five-membered ring polyamide **4** binds preferentially to the site 5'-TGTTTA-3' as expected, revealing a preference for the T•A base pair by **Hp/Py**. The binding affinity determined for the T•A and A•T sites were $K_a = 4.1 \times 10^8 \text{ M}^{-1}$, and $K_a \leq 2 \times 10^7 \text{ M}^{-1}$, respectively, a specificity of at least 20-fold. No binding was detected in the concentration range up to 200 nM for the two G•C and C•G sites. Remarkably, analysis of the hydroxybenzimidazole-containing polyamide **3** showed that this hairpin binds with similar affinity and specificity as **4**. Polyamide **3** binds the site 5'-TGTTTA-3' with an affinity of $K_a = 5.7 \times 10^8 \text{ M}^{-1}$, an 18-fold selectivity of T•A over A•T. The sequence 5'-TGTGTA-3', representing a G•C mismatch site, was bound with at least 80-fold lower affinity. No binding was observed for the C•G mismatch site. Thus, sequence specificity can be

(19) Trauger, J. W.; Dervan, P. B. *Methods Enzymol.* **2001**, *340*, 450–466.

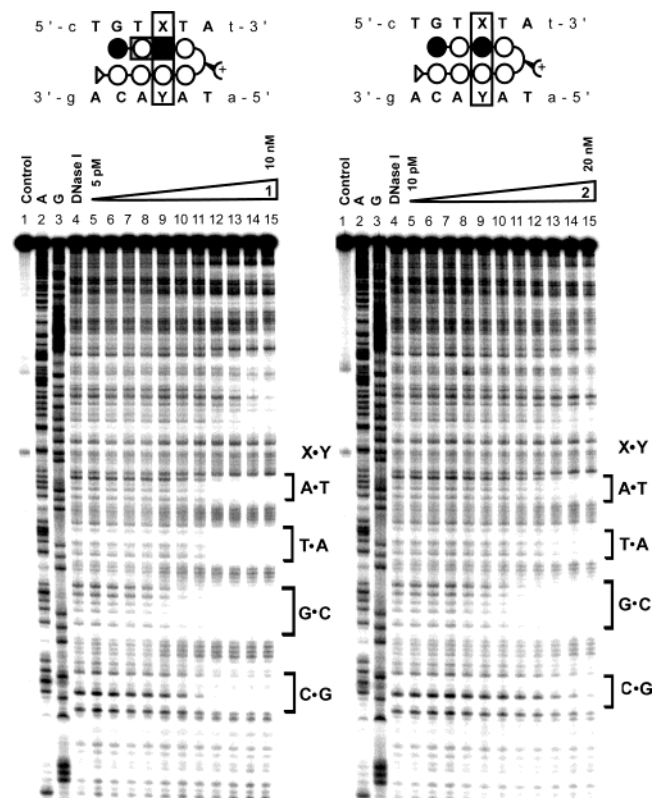


Figure 5. Quantitative DNase I footprint titration experiments on the 3'-³²P-labeled 284-bp *EcoRI/PvuII* restriction fragment from plasmid pDR1. Left: polyamide **1**: lane 1, intact DNA; lane 2, A-specific reaction; lane 3, G-specific reaction; lane 4, DNase I standard; lane 5–15, 5, 10, 20, 50, 100, 200, 500 pM and 1, 2, 5, 10 nM polyamide, respectively. Right: polyamide **2**: lane 1, intact DNA; lane 2, A-specific reaction; lane 3, G-specific reaction; lane 4, DNase I standard; lane 5–15, 10, 20, 50, 100, 200, 500 pM and 1, 2, 5, 10, 20 nM polyamide, respectively. The analyzed 6-base pair binding site locations are designated in brackets along the right side of each autoradiogram with their respective unique base pairs indicated. Schematic binding models of **1** and **2** with their putative binding sites are shown on the top side of the autoradiograms. Flanking sequences are designated in lower case, regular type, while the binding site is given in capital bold type. The boxed **X•Y** base pair indicates the position that was examined in the experiments.

retained by replacing an **Hp** with an **H_z** unit. Presumably the T•A selectivity arises in this DNA sequence context in part from shape selection in the minor groove by the phenolic OH group against the O(2) of thymine versus the C(2)–H of adenine. Importantly, the hydroxybenzimidazole-containing polyamide **3** is stable at acidic pH.

Benzimidazole/Pyrrole Pair. To complete this study a third polyamide containing the benzimidazole building block was included. This would allow a comparison of the specificity of **Bi/Py** pairs with **Py/Py** pairs and serve as a control as well, confirming that the different specificity of **H_z/Py** vs **Bi/Py** is due to the single atomic substitution of CH to COH on the benzene ring (Table 2. For the all five-membered ring polyamide **6** the DNA binding affinity is highest at match sites 5'-TGTTTA-3' and 5'-TGTATA-3' within a factor of 2. The binding affinity to the G•C and C•G sites is lower by a factor of 23. The same binding site preference was also found for the benzimidazole containing polyamide **5** revealing that **Bi/Py** mimics **Py/Py** and binds both A•T and T•A.

Several factors are considered to play a role in stabilizing ligand interactions in the minor groove of DNA. Hydrogen bonding, shape complementarity and electrostatic interactions

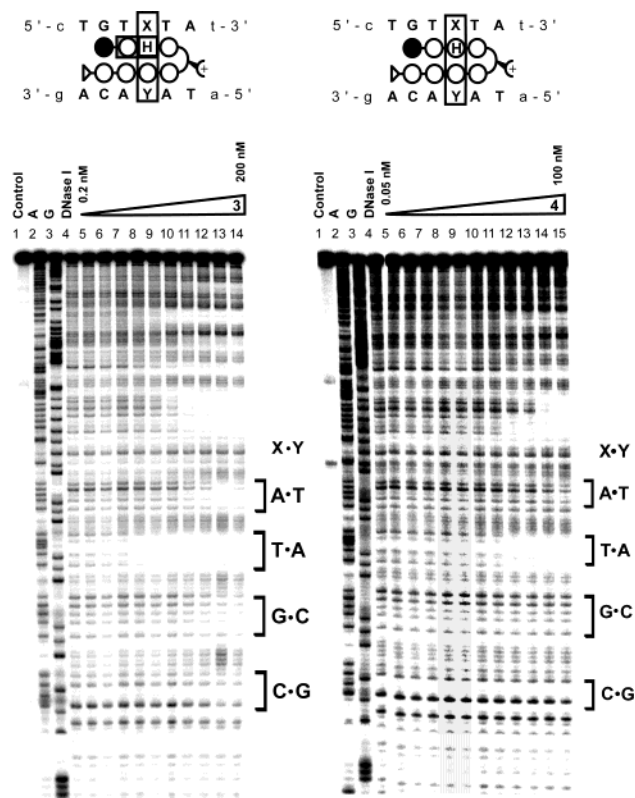


Figure 6. Quantitative DNase I footprint titration experiments on the 3'-³²P-labeled 284-bp *EcoRI/PvuII* restriction fragment from plasmid pDR1. Left: polyamide **3**: lane 1, intact DNA; lane 2, A-specific reaction; lane 3, G-specific reaction; lane 4, DNase I standard; lane 5–14, 0.2, 0.5, 1, 2, 5, 10, 20, 50, 100, 200 nM polyamide, respectively. Right: polyamide **4**: lane 1, intact DNA; lane 2, A-specific reaction; lane 3, G-specific reaction; lane 4, DNase I standard; lane 5–15, 0.05, 0.1, 0.2, 0.5, 1, 2, 5, 10, 20, 50, 100 nM polyamide, respectively. The analyzed 6-base pair binding site locations are designated in brackets along the right side of each autoradiogram with their respective unique base pairs indicated. Schematic binding models of **3** and **4** with their putative binding sites are shown on the top side of the autoradiograms. Flanking sequences are designated in lower case, regular type, while the binding site is given in capital bold type. The boxed **X•Y** base pair indicates the position that was examined in the experiments.

are major contributors. Fused heterocycle subunits, such as imidazo[4,5-*b*]pyridine-pyrrole or hydroxybenzimidazole-pyrrole, are conformationally restricted compared with bis-pyrrololecarboxamides leading to entropically stabilized complexes with DNA. Because Ip and H_z contain one amide linkage less than their respective distamycin analogues, the resulting higher hydrophobicity of the curved ligand with a different hydration behavior could contribute to a deeper position of the polyamide in the minor groove allowing stronger hydrogen bonding and van der Waals interactions with the floor and walls of the DNA groove.

Inspection of the curvature of **Ip**-, **H_z**-, and **Bi**-containing polyamides as obtained from gas-phase calculations of ImPyXPy fragments, where X = **Ip**, **H_z**, and **Bi** compared to their parent fragments ImPyXPy, where X = **Im**, **Hp**, and **Py** indicate that the strands bearing a six-membered fused heterocycle have a smaller degree of curvature than the corresponding five-membered ring systems (see Supporting Information Figures S1, S2, S3). Due to the fact that hairpin polyamides containing **Im**, **Hp**, and **Py** are slightly over-curved with respect to the DNA helix, one could assume that the **Ip**-, **H_z**-, or **Bi**-containing

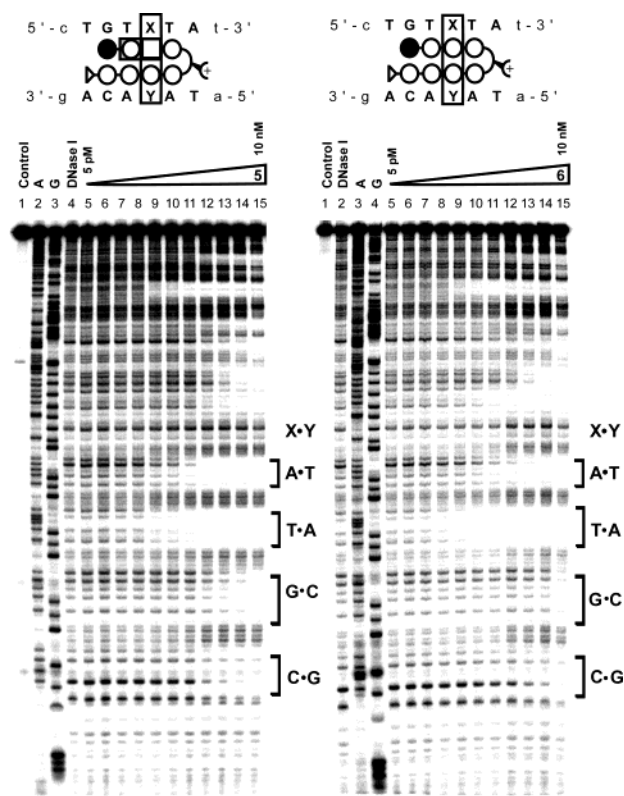


Figure 7. Quantitative DNase I footprint titration experiments on the 3'-³²P-labeled 284-bp *EcoRI/PvuII* restriction fragment from plasmid pDR1. Left: polyamide **5**: lane 1, intact DNA; lane 2, A-specific reaction; lane 3, G-specific reaction; lane 4, DNase I standard; lane 5–15, 5, 10, 20, 50, 100, 200, 500 pM and 1, 2, 5, 10 nM polyamide, respectively. Right: polyamide **6**: lane 1, intact DNA; lane 2, DNase I; lane 3, A-specific reaction; lane 4, G-specific reaction; lane 5–15, 5, 10, 20, 50, 100, 200, 500 pM and 1, 2, 5, 10 nM polyamide, respectively. The analyzed 6-base pair binding site locations are designated in brackets along the right side of each autoradiogram with their respective unique base pairs indicated. Schematic binding models of **5** and **6** with their putative binding sites are shown on the top side of the autoradiograms. Flanking sequences are designated in lower case, regular type, while the binding site is given in capital bold type. The boxed **X•Y** base pair indicates the position that was examined in the experiments.

strand of the hairpin polyamides **1**, **3**, and **5** have a better shape complementarity with the minor groove of DNA. Indeed, the increased DNA binding affinity of the polyamides comprising Ip, Hz, or Bi units might be a result of the decreased curvature and therefore deeper position into the minor groove. Nevertheless, in this first exploratory study only one strand of the hairpin was substituted, whereas the opposite one remained five-membered rings. On the basis of the data presented here, it will be interesting to examine whether antiparallel unsymmetrical pairs of the benzimidazole analogues, **Ip/Bi** and **Hz/Bi**, mimic **Im/Py** and **Hp/Py**, and code for G•C and T•A base pairs, respectively.

Conclusion

Six-membered ring heterocycles **Ip**, **Hz**, and **Bi**, paired opposite the five-membered ring **Py**, bind the minor groove of DNA and distinguish the edges of the four Watson–Crick base pairs. The **Ip/Py** pair mimics an **Im/Py** and exhibits the same preference for G•C. The **Bi/Py** pair mimics **Py/Py** and exhibits the same preferences for A/T vs G/C base pairs. Most importantly, the **Hz/Py** pair distinguishes a T•A base pair from an A•T base pair and is a strong candidate to replace **Hp/Py** in

our biological gene regulation studies. The DNA binding properties of polyamides containing multiple **Hz/Py** pairs, as well structural studies, will be reported in due course.







Experimental Section

General. ¹H NMR and ¹³C NMR spectra were recorded on a Varian Mercury 300 and 500 instrument. Chemical shift values were recorded as parts per million relative to solvent and coupling constants in hertz. All NMR spectra were measured at room temperature (unless otherwise stated). UV spectra were measured on a Beckman Coulter DU 7400 diode array spectrophotometer. Mass spectra were recorded on the following mass spectrometer: matrix-assisted, laser desorption/ionization time-of-flight (MALDI-TOF) on Voyager DE-PRO from Applied Biosystems, fast atom bombardment (FAB) on a JEOL JMS-600H double focusing high-resolution magnetic sector, and electrospray injection (ESI) LCQ ion trap on a LCQ classic, ThermoFinnigan and were carried out at the Protein and Peptide Microanalytical Facility at the California Institute of Technology. Precoated plates silica gel 60F₂₅₄ (Merck) were used for TLC and silica gel 60 (40 μm) for flash chromatography. Visualization was realized by UV and/or by using a solution of Ce(SO₄)₂, phosphomolybdic acid, H₂SO₄, and H₂O. HPLC analysis was performed on a Beckman Gold system using a Varian C₁₈, Microsorb-MV 100–5, 250 × 4.6 mm reversed-phase column in 0.1% (w/v) TFA with acetonitrile as eluent and a flow rate of 1.0 mL/min, gradient elution 1.25% acetonitrile/min. Preparatory HPLC was carried out on a Beckman HPLC using a Waters DeltaPak 100 × 25 mm, 100 μm C₁₈ column, 0.1% (w/v) TFA, 0.25% acetonitrile/min. 18 MΩ water was obtained from a Millipore MilliQ water purification system, and all buffers were 0.2 μm filtered. DNA oligonucleotides were synthesized by the Biopolymer Synthesis Center at the California Institute of Technology and used without further purification. Plasmids were sequenced by the Sequence/Structure Analysis Facility (SAF) at the California Institute of Technology. DNA manipulations were performed according to standard protocols. Autoradiography was performed with a Molecular Dynamics Typhoon Phosphorimager. Reactions were carried out under Ar in anhydrous solvents. *N,N'*-Dicyclohexylcarbodiimide (DCC), *N*-hydroxybenzotriazole (HOBt), and 2-(1*H*-benzotriazole-1-yl)-1,1,3,3-tetramethyluronium hexafluorophosphate (HBTU) were purchased from Peptides International. Oxime resin was purchased from Novabiochem (0.48 mmol/g). (*R*)-2-Fmoc-4-Boc-diaminobutyric acid (α-Fmoc-γ-Boc-(*R*)-DABA, **29**) was from Bachem, dichloromethane (DCM) was reagent grade from EM, and trifluoroacetic acid (TFA) was from Halocarbon. Bis(triphenylphosphine)palladium(II)dichloride was from Fluka, all other reagents were from Aldrich (highest quality available). All enzymes (unless otherwise stated) were purchased from Roche Diagnostics and used with their supplied buffers. pUC19 was from New England Biolabs. [α-³²P]-Deoxyadenosine triphosphate and [α-³²P]-thymine triphosphate was purchased from New England Nucleotides. RNase-free water (used for all DNA manipulations) was from US Biochemicals. Ethanol (200 proof) was from Equistar, 2-propanol from Mallinckrodt. Premixed tris-borate-EDTA (Gel-Mate, used for gel running buffer) was from Gibco. Bromophenol blue and xylene cyanol FF were from Acros. 3-Methoxy-1-methyl-4-nitro-1*H*-pyrrole-2-carboxylic acid (**11**) was synthesized as reported earlier.¹¹

Monomer Syntheses. 2-Amino-3-nitro-6-bromo-pyridine (**8**) was synthesized in 2 steps following described procedures.^{13,14} Data of **8**: *R*_f 0.30 (hexane/EtOAc 1:1). ¹H NMR (300 MHz, DMSO-*d*₆): δ 6.87 (d, *J* = 8.2 Hz, 1H), 8.23 (d, *J* = 8.2 Hz, 1H), 8.25 (brs, 2H).

6-Amino-5-nitro-pyridine-2-carboxylic Acid Methyl Ester (9). To a solution of bromide **8** (8.0 g, 36.6 mmol) in DMF (130 mL) were added methanol (130 mL), Pd(OAc)₂ (248 mg, 1.1 mmol), triphenylphosphine (316 mg, 1.2 mmol) and Et₃N (20 mL). The mixture was stirred for 10 min and then transferred into a parr apparatus. After evacuating 3 times with CO, the reaction mixture was heated under a CO pressure of 15 atm to 60 °C for 15 h. The red/brown solution was

Table 1. Equilibrium Association Constants K_a [M^{-1}] for Polyamides **1**, **2**, **3**, **4**, **5**, and **6**

| Polyamide | 5'-cTGTATAt-3' | 5'-cTGTTTAt-3' | 5'-cTGTGTAt-3' | 5'-cTGTCTAt-3' |
|---|---------------------------------------|------------------------------------|---------------------------------------|------------------------------------|
|  1 | $3.7 \times 10^9 (\pm 0.4)$ [3] | $2.3 \times 10^9 (\pm 0.4)$ [5] | $1.2 \times 10^{10} (\pm 0.2)$ | $5.4 \times 10^9 (\pm 1.5)$ [2] |
|  2 | $5.5 \times 10^8 (\pm 0.3)$ [4] | $2.9 \times 10^8 (\pm 0.2)$ [8] | $2.3 \times 10^9 (\pm 0.3)$ | $2.7 \times 10^8 (\pm 0.4)$ [9] |
|  3 | $3.1 \times 10^7 (\pm 0.9)$ [18] | $5.7 \times 10^8 (\pm 0.4)$ | $\leq 7 \times 10^6$ [≥ 80] | / |
|  4 | $\leq 2 \times 10^7$ [≥ 20] | $4.1 \times 10^8 (\pm 1.4)$ | / | / |
|  5 | $7.8 \times 10^9 (\pm 0.8)$ [2] | $1.1 \times 10^{10} (\pm 0.1)$ | $1.4 \times 10^9 (\pm 0.3)$ [8] | $2.6 \times 10^9 (\pm 0.3)$ [4] |
|  6 | $3.3 \times 10^9 (\pm 1.1)$ [2] | $6.9 \times 10^9 (\pm 0.8)$ | $\leq 3 \times 10^8$ [≥ 23] | $8.6 \times 10^8 (\pm 0.7)$ [8] |

^a The reported association constants K_a are the average values obtained from three DNase I footprint titration experiments, with the standard deviation for each data set indicated in parentheses. ^b The assays were carried out at 22 °C at pH 7.0 in the presence of 10 mM Tris-HCl, 10 mM KCl, 10 mM MgCl₂, and 5 mM CaCl₂ with an equilibration time of 12 h. ^c Specificities are given in brackets under the K_a values and calculated as $K_a(\text{match})/K_a(\text{mismatch})$.

Table 2. Specificity of Bi, Hz, and Ip Pairings^a

| pair | T-A | A-T | G-C | C-G |
|-------|-----|-----|-----|-----|
| Bi/Py | + | + | — | — |
| Hz/Py | + | — | — | — |
| Ip/Py | — | — | + | — |

^a Favored (+), disfavored (—).

then cooled to r.t., filtered through a pad of Celite, rinsed with EtOAc and concentrated. Purification by flash chromatography (hexane/EtOAc 1:1) afforded 4.4 g (61%) of **9** as a bright yellow solid. Data of **9**: R_f 0.57 (hexane/EtOAc 1:1). ¹H NMR (300 MHz, DMSO-*d*₆): δ 3.85 (s, 3H), 7.27 (d, J = 8.8 Hz, 1H), 8.09 (brs, 2H), 8.52 (d, J = 8.8 Hz, 1H). ¹³C NMR (75 MHz, DMSO-*d*₆): δ 53.52, 113.10, 129.43, 137.48, 152.41, 153.79, 164.53. MS (ESI): m/z (rel intensity) 198 (100).

5,6-Diamino-pyridine-2-carboxylic Acid Methyl Ester (10). Methyl ester **9** (3.5 g, 18.0 mmol) was dissolved in methanol (300 mL) and EtOAc (300 mL) and the solution was degassed with Ar. After the addition of Pd/C (10 wt %, 0.7 g) the reaction mixture was stirred for 4 h under a hydrogen atmosphere. Filtration through a pad of Celite with EtOAc, evaporation of the solvent and purification by flash chromatography (EtOAc/MeOH 15:1) yielded 2.4 g (79%) of **10** as a deep red powder. Data of **10**: R_f 0.42 (EtOAc/MeOH 15:1). ¹H NMR (300 MHz, DMSO-*d*₆): δ 3.68 (s, 3H), 5.51 (brs, 2H), 5.78 (brs, 2H), 6.67 (d, J = 7.7 Hz, 1H), 7.21 (d, J = 7.7 Hz, 1H). ¹³C NMR (75 MHz, DMSO-*d*₆): δ 51.88, 116.32, 117.98, 132.40, 135.09, 147.93, 166.30. MS (ESI): m/z (rel intensity) 168 (100).

5-Amino-6-[(1-methyl-4-nitro-1H-pyrrole-2-carbonyl)-amino]-pyridine-2-carboxylic acid methyl ester and 6-amino-5-[(1-methyl-4-nitro-1H-pyrrole-2-carbonyl)-amino]-pyridine-2-carboxylic acid methyl ester (12a/12b). Carboxylic acid **11** (2.0 g, 11.8 mmol) and diamine **10** (1.8 g, 10.8 mmol) were dissolved in DMF (26 mL). 2-(1H-benzotriazole-1-yl)-1,1,3,3-tetramethyluronium hexafluorophosphate (HBTU) (4.4 g, 11.2 mmol) and *N,N*-diisopropylethylamine (DIEA)

(2.5 mL) were added and the mixture was stirred under heating to 40 °C for 2 days. The reaction mixture was poured into ice and the precipitate formed was collected by filtration. Drying under hv provided 2.8 g (82%) as a mixture of both isomers **12a** and **12b** in a ratio of 3:2 (as determined by ¹H NMR) as a red/brown solid which were used without separation. Data of **12a** and **12b**: R_f 0.55, 0.65 (hexane/EtOAc 1:5). ¹H NMR (300 MHz, DMSO-*d*₆): δ 3.76, 3.79, 3.91, 3.92 (4s, 6H), 5.99 (brs, 0.6H), 6.35 (brs, 0.4H), 7.10 (d, J = 8.2 Hz, 0.6H), 7.30 (d, J = 8.2 Hz, 0.4H), 7.72–7.77 (m, 4H), 8.21 (s, 2H), 9.59 (brs, 0.4H), 10.33 (brs, 0.6H). ¹³C NMR (75 MHz, DMSO-*d*₆): δ 38.27, 38.45, 52.32, 52.70, 109.73, 109.90, 114.54, 119.42, 121.69, 121.95, 126.18, 126.62, 129.04, 129.13, 132.86, 133.59, 134.46, 136.23, 142.80, 144.78, 159.54, 162.87, 165.43, 165.83. MS (ESI): m/z (rel intensity) 320 (65). HRMS (FAB): m/z calcd for C₁₃H₁₄N₅O₅, 320.0987; found, 320.0994.

2-(4-tert-Butoxycarbonylamino-1-methyl-1H-pyrrole-2-yl)-3H-imidazo[4,5-*b*]pyridine-5-carboxylic Acid Methyl Ester (14). The aforementioned mixture of amino amides **12a** and **12b** (0.80 g, 2.4 mmol) was suspended in glacial acetic acid (20 mL) and heated to 80 °C for 7 h. The redish/grey suspension was then concentrated and dried under hv to obtain crude **13** as a brown solid in a ca. 1:1 mixture with unreacted amino amide **12a** (as determined with ¹H NMR). Data of **13**: R_f 0.62 (hexane/EtOAc 1:5). ¹H NMR (300 MHz, DMSO-*d*₆): δ 3.86 (s, 3H), 3.92 (s, 3H), 7.40 (d, J = 8.2, 1H), 7.98 (d, J = 2.2, 1H), 8.26 (d, J = 1.6, 1H), 8.41 (d, J = 8.2, 1H), 10.26 (s, 1H). MS (ESI): m/z (rel intensity) 302 (13).

To a solution of unpurified **13** (0.75 g, 2.5 mmol) in DMF (13 mL) was added SnCl₂·2H₂O (3.4 g, 15.0 mmol) and the mixture was stirred under heating to 50 °C for 36 h. After completion of the reaction detected by TLC, Boc₂O (830 mg, 3.7 mmol) and DIEA (0.4 mL) were added to the reaction mixture. After stirring for 20 h another portion of Boc₂O (280 mg, 1.25 mmol) was added and stirring was continued for an additional 18 h. The mixture was concentrated, the residue redissolved in EtOAc, and washed with brine. The organic phase was

dried over MgSO_4 and the solvent evaporated. Flash chromatography (hexane/EtOAc 1:4) afforded 130 mg (14%, 3 steps, based on **12a/12b**) of **14** as a yellow powder. Data of **14**: R_f 0.45 (hexane/EtOAc 1:4). Compound **14** appears as two tautomers (1H/3H) on the NMR time scale at r.t. in a ratio of about 1:1;²¹ heating the NMR probe to 70 °C results in only one set of signals. UV (MeOH): λ_{max} 364. ^1H NMR (300 MHz, DMSO- d_6 , 70 °C): δ 1.43 (s, 9H), 3.85 (s, 3H), 4.04 (s, 3H), 6.94 (brs, 2H, D₂O exchange), 7.08 (brs, 1H), 7.88–7.97 (m, 3H), 9.24 (s, 2H, D₂O exchange). ^{13}C NMR (75 MHz, DMSO- d_6): δ 28.85, 31.95, 37.42, 52.81, 79.07, 86.25, 104.53, 118.52, 119.90, 125.39, 146.79, 151.23, 153.37. MS (ESI): m/z (rel intensity) 372 (100). HRMS (FAB): m/z calcd for $\text{C}_{18}\text{H}_{22}\text{N}_5\text{O}_4$, 372.1671; found, 372.1660.

2-(4-tert-Butoxycarbonylamino-1-methyl-1H-pyrrole-2-yl)-3H-imidazo[4,5-b]pyridine-5-carboxylic acid (15). Compound **14** (60 mg, 0.6 mmol) was dissolved in 0.2 M NaOH in H₂O/dioxane 1:1 (7 mL) and stirred for 5 h at r.t. while the solution turned orange. The solution was cooled to 0 °C and 1N HCl was added dropwise until pH 1–2, while an orange precipitate developed. The product was separated by centrifugation, the supernatant removed, and the formed precipitate washed with cold H₂O (2 × 2 mL). Lyophilization afforded 46 mg (81%) of **15** as an orange solid. Data of **15**: UV (MeOH): λ_{max} 359. ^1H NMR (300 MHz, DMSO- d_6): δ 1.46 (s, 9H), 4.05 (s, 3H), 7.01 (brs, 1H, D₂O exchange), 7.15 (s, 1H), 7.98 (m, 3H), 9.30 (s, 1H, D₂O exchange). ^{13}C NMR (75 MHz, DMSO- d_6): δ 28.96, 37.47, 79.21, 106.38, 118.65, 119.93, 120.44, 122.32, 124.99, 141.58, 150.32, 153.38, 166.53. MS (ESI): m/z (rel intensity) 358 (100). HRMS (FAB): m/z calcd for $\text{C}_{17}\text{H}_{20}\text{N}_5\text{O}_4$, 358.1515; found, 358.1506.

4-Acetylamino-5-chloro-2-methoxy-3-nitro-benzoic Acid Methyl Ester (17). The title compound was synthesized according to a literature procedure applying some modifications.¹⁸ Fuming nitric acid (33 mL) was added dropwise at 20 °C to compound **16** (13.0 g, 0.05 mol) over 15 min. After stirring for an additional 10 min at that temperature, the mixture was poured into ice water and EtOAc (100 mL) was added. After separating the organic phase, the aqueous phase was extracted with EtOAc. The combined organic phases were washed with brine, dried over MgSO_4 and concentrated. Drying under hv yielded 14.0 g (91%) of **17** as a beige solid. ^1H NMR (300 MHz, DMSO- d_6): δ 2.01 (s, 3H), 3.84 (s, 3H), 3.87 (s, 3H), 8.12 (s, 1H), 10.30 (s, 1H).

4-Amino-5-chloro-2-methoxy-3-nitro-benzoic Acid Methyl Ester (18). Compound **17** (6.2 g, 20.5 mmol) was dissolved in methanol (70 mL), H₂SO₄ concentrated (4 mL) was added and the solution heated to reflux for 9 h. After cooling to r.t., the mixture was poured into ice (600 mL) and the precipitate formed was collected by filtration. Drying under hv gave 5.0 g (94%) of **18** as a yellow solid. Data of **18**: R_f 0.85 (hexane/EtOAc 1:4). ^1H NMR (300 MHz, DMSO- d_6): δ 3.77 (s, 6H), 6.85 (brs, 2H), 7.82 (s, 1H). ^{13}C NMR (75 MHz, DMSO- d_6): δ 52.80, 64.68, 110.40, 114.21, 133.80, 142.29, 153.60, 163.48. MS (ESI): m/z (rel intensity) 261 (100). HRMS (FAB): m/z calcd for $\text{C}_9\text{H}_9\text{N}_2\text{O}_5\text{Cl}$, 260.0200; found, 260.0197.

3,4-Diamino-2-methoxy-benzoic Acid Methyl Ester (19). Amine **18** (4.8 g, 18.4 mmol) was dissolved in methanol (250 mL) and the resulting solution was intensively degassed for 10 min with Ar. Pd/C (10 wt %, 4.5 g) was added, followed by Et₃N (30 mL) and the resulting mixture was transferred to a parr apparatus. After being stirred for 6 h under a hydrogen atmosphere at 5 atm, the reaction mixture was filtered through a pad of Celite and rinsed with methanol. Evaporation of the solvent yielded crude diamine **19** as a brown gum (with residual Et₃N). Data for **19**: R_f 0.43 (hexane/EtOAc 1:4). ^1H NMR (300 MHz, DMSO- d_6): δ 3.62 (s, 3H), 3.67 (s, 3H), 4.38 (brs, 2H), 5.38 (brs, 2H), 6.30 (d, J = 8.2 Hz, 1H), 6.96 (d, J = 8.2 Hz, 1H). ^{13}C NMR (75 MHz,

DMSO- d_6): δ 51.77, 60.53, 109.36, 111.27, 121.35, 127.78, 141.95, 147.61. MS (ESI): m/z (rel intensity) 197 (55).

4-Amino-2-methoxy-3-[(1-methyl-4-nitro-1H-pyrrole-2-carbonyl)-amino]-benzoic Acid Methyl Ester (20a/20b). Carboxylic acid **11** (3.0 g, 17.6 mmol) and the aforementioned crude diamine **19** were dissolved in DMF (50 mL). HBTU (6.5 g, 16.5 mmol) and DIEA (3.4 mL) were added, and the reaction mixture was stirred for 1.5 days. The mixture was poured into ice and the precipitate collected by filtration. After washing with cold water and drying under hv provided 4.4 g (68%) as a mixture of the two isomeric amino amides **20a/20b** in a ratio of about 1:1 (as determined by ^1H NMR) as a beige solid. Data of **20a** and **20b**: R_f 0.58, 0.74 (hexane/EtOAc 1:4). ^1H NMR (300 MHz, DMSO- d_6): δ 3.61, 3.69, 3.75, 3.90 (4s, 9H), 5.04 (brs, 1H), 5.89 (brs, 1H), 6.47 (d, J = 8.1 Hz, 0.5H), 6.94 (d, J = 8.2 Hz, 0.5H), 7.09 (d, J = 8.2 Hz, 0.5H), 7.49 (d, J = 8.1 Hz, 0.5H), 7.63–7.69 (m, 1H), 8.17–8.20 (m, 1H), 9.30 (brs, 0.5H), 9.65 (brs, 0.5H). ^{13}C NMR (75 MHz, DMSO- d_6): δ 38.18, 38.30, 51.98, 52.67, 61.23, 62.01, 108.98, 109.54, 110.07, 110.38, 115.48, 117.35, 121.92, 122.19, 127.19, 128.57, 131.83, 134.44, 147.52, 152.26, 159.57, 160.08, 165.67, 166.49. MS (ESI): m/z (rel intensity) 349 (100). HRMS (FAB): m/z calcd for $\text{C}_{15}\text{H}_{16}\text{N}_4\text{O}_6$, 348.1069; found, 348.1085.

4-Methoxy-2-(1-methyl-4-nitro-1H-pyrrol-2-yl)-3H-benzimidazole-5-carboxylic Acid Methyl Ester (21). The aforementioned mixture of amides **20a/20b** (500 mg, 1.43 mmol) was suspended in glacial acetic acid (8 mL) and heated to 90 °C for 7 h. Most of the solvent was evaporated, and the yellow residue was suspended in Et₂O. After being vigorously stirred for 20 min, the precipitate was filtered and washed with Et₂O. Drying under hv gave 404 mg (85%) of **21** as a beige solid. Data of **21**: R_f 0.80 (hexane/EtOAc 1:5). ^1H NMR (300 MHz, DMSO- d_6): δ 3.76 (s, 3H), 4.14 (s, 3H), 4.34 (s, 3H), 7.14–7.17 (m, 1H), 7.48–7.55 (m, 3H), 8.25 (s, 1H). MS (ESI): m/z (rel intensity) 331 (98).

2-(4-tert-Butoxycarbonylamino-1-methyl-1H-pyrrol-2-yl)-4-methoxy-3H-benzimidazole-5-carboxylic Acid Methyl Ester (22). Compound **21** (400 mg, 1.21 mmol) was dissolved in DMF (10 mL) and Pd/C (10 wt %, 150 mg) was added. The mixture was transferred into a parr apparatus and stirred for 5 h under a hydrogen atmosphere of 10 atm. After the TLC revealed no starting material, the mixture was transferred into a round-bottom flask and Boc₂O (400 mg, 1.81 mmol) and DIEA (0.5 mL) were directly added. The reaction mixture was stirred overnight, filtered through a pad of Celite, rinsed with EtOAc, and concentrated in vacuo. Purification by flash chromatography (hexane/EtOAc 1:2) afforded 248 mg (51%) of **22** as a beige solid. Data of **22**: R_f 0.34 (hexane/EtOAc 1:2). ^1H NMR (300 MHz, DMSO- d_6): δ 1.43 (s, 9H), 3.75 (s, 3H), 3.99 (s, 3H), 4.31 (s, 3H), 6.78 (s, 2H, CH, D₂O exchange), 6.95 (s, 1H), 7.05 (d, J = 8.2 Hz, 1H), 7.45 (d, J = 8.6 Hz, 1H), 9.18 (brs, 1H, D₂O exchange). ^{13}C NMR (75 MHz, DMSO- d_6): δ 28.62, 38.20, 51.98, 62.01, 108.98, 110.08, 115.48, 127.19, 128.57, 131.84, 152.25, 160.09, 165.67. UV (MeOH): λ_{max} 327. MS (ESI): m/z (rel intensity) 401 (100).

2-(4-tert-Butoxycarbonylamino-1-methyl-1H-pyrrol-2-yl)-4-methoxy-3H-benzimidazole-5-carboxylic Acid (23). Methyl ester **22** (51 mg, 0.13 mmol) was dissolved in 1 M NaOH (1:1 dioxane/H₂O, 5 mL) and stirred overnight at r.t. and an additional 3 h at 50 °C. The reaction mixture was cooled to 0 °C and 1N HCl was added dropwise to adjust the pH to 3–4, while a white precipitate was formed. Separation of the product was accomplished by centrifugation and decanting of the supernatant. Lyophilization gave 36 mg (73%) of **23** as a beige solid. Data of **23**: ^1H NMR (500 MHz, DMSO- d_6): δ 1.40 (s, 9H), 3.97 (s, 3H), 4.28 (s, 3H), 6.76 (s, 1H), 6.92 (s, 1H), 7.02 (d, J = 8.2 Hz, 1H), 7.44 (d, J = 8.2 Hz, 1H), 9.13 (s, 1H), 12.20 (brs, 1H). ^{13}C NMR (125 MHz, DMSO- d_6): δ 27.80, 36.34, 60.78, 78.29, 102.88, 104.47, 114.67, 116.12, 119.79, 123.54, 124.96, 135.00, 139.02, 145.90, 150.62, 152.78, 167.70. UV (H₂O): λ_{max} 319. MS (ESI): m/z (rel intensity) 387 (100). HRMS (FAB): calcd for $\text{C}_{19}\text{H}_{23}\text{N}_4\text{O}_5$, 387.1668; found, 387.1658.

(20) Besides the designed four binding sites there are several overlapping 1-base pair and 2-base pair mismatch sites present on the plasmid to which polyamides **3** and **4** show comparable binding behavior.

(21) Troschütz, R.; Lückel, A. *Arch. Pharm.* **1992**, 325, 617–619.

(22) (a) Iverson, B. L.; Dervan, P. B. *Nucl. Acids Res.* **1987**, 15, 7823–7830. (b) Maxam, A. M.; Gilbert, W. S. *Methods Enzymol.* **1980**, 65, 499–560.

Polyamide Syntheses. Polyamides **2**, **4**, **6** were synthesized in a stepwise fashion from 0.48 mmol/g oxime resin by manual solid-phase methods using Boc-protected amino acid building blocks as reported earlier.¹² The incorporation of the imidazo[4,5-*b*]pyridine, hydroxybenzimidazole and benzimidazole Boc-protected building blocks, to synthesize polyamides **1**, **3**, and **5**, was realized under identical conditions. Activation of **15**, **23**, **24** was achieved with HBTU (1 eq. in NMP, DIEA) for 10 min and coupling was realized for 3 h at r.t. Deprotection of the immobilized polyamides-containing building blocks was successful using 20% TFA in CH₂Cl₂ for 25 min.

Extinction coefficients were calculated based on $\epsilon = 8690 \text{ cm}^2 \text{ L mol}^{-1}$ per ring at 310 nm for the polyamides **2**, **4**, and **6**.¹⁹ The extinction coefficient for polyamides **1**, **3**, and **5** was determined as $28\,500 \text{ cm}^2 \text{ L mol}^{-1}$ (at 330 nm), $33\,914 \text{ cm}^2 \text{ L mol}^{-1}$ (at 318 nm), and $40\,081 \text{ cm}^2 \text{ L mol}^{-1}$ (at 326 nm), respectively.

Procedure for MeNH₂ Cleavage from the Resin.^{12b} After completion of the synthesis of the polyamides the resin was filtered off the reaction and washed with DMF, DCM, MeOH, Et₂O, and dried in vacuo. A sample of the resin (150 mg) was swollen in DCM (3 mL) and treated with MeNH₂ (2M in THF, 3 mL) under periodic agitation at 37 °C for 16 h. The resin was then removed by filtration, washed with DCM and DMF, and concentrated in vacuo. After diluting with 20% MeCN/0.1% TFA the crude mixture was purified by preparative reversed-phase HPLC to yield the pure polyamides.

ImPyIpPy-(R)^H2^Nγ-PyPyPyPy-CONHMe (1). Starting with 100 mg of resin the title compound was synthesized. It was recovered upon lyophilization of the appropriate fractions as an orange powder (0.4 mg). UV (H₂O): λ_{max} 375, 330, 248. MALDI-TOF-MS: calcd. for C₅₂H₅₇N₂₀O₈, 1090.1; found, 1090.1, 1110.8 (M+Na).

ImPyImPy-(R)^H2^Nγ-PyPyPyPy-CONHMe (2). Starting with 150 mg of resin the title compound was synthesized. It was recovered upon lyophilization of the appropriate fractions as a white powder (0.5 mg). UV (H₂O): λ_{max} 314, 246. MALDI-TOF-MS: calcd. for C₅₁H₅₉N₂₀O₉, 1096.1; found, 1096.1, 1117.1 (M+Na).

ImPyBiPy-(R)^H2^Nγ-PyPyPyPy-CONHMe (5). Starting with 150 mg of resin the title compound was synthesized. It was recovered upon lyophilization of the appropriate fractions as a beige powder (0.6 mg). UV (H₂O): λ_{max} 326, 246. MALDI-TOF-MS: calcd. for C₅₃H₅₈N₁₉O₈, 1089.1; found, 1089.1.

ImPyPyPy-(R)^H2^Nγ-PyPyPyPy-CONHMe (6). Starting with 150 mg of resin the title compound was synthesized. It was recovered upon lyophilization of the appropriate fractions as a white powder (0.7 mg). UV (H₂O): λ_{max} 316, 246. MALDI-TOF-MS: calcd. for C₅₂H₅₉N₁₉O₉, 1094.1; found, 1094.2.

ImPyOzPy-(R)^H2^Nγ-PyPyPyPy-CONHMe (31). Starting with 200 mg of resin the title compound was synthesized. It was recovered upon lyophilization of the appropriate fractions as a white powder (1.6 mg). UV (H₂O): λ_{max} 320, 246. MALDI-TOF-MS: calcd. for C₅₄H₆₀N₁₉O₉, 1119.1; found, 1119.2, 1142.17 (M+Na).

ImPyOpPy-(R)^H2^Nγ-PyPyPyPy-CONHMe (32). Starting with 200 mg of resin the title compound was synthesized. It was recovered upon lyophilization of the appropriate fractions as a white powder (0.8 mg). UV (H₂O): λ_{max} 318, 245. MALDI-TOF-MS: calcd. for C₅₃H₆₂N₁₉O₁₀, 1125.1; found, 1125.6.

Deprotection of the *O*-Methyl-Protected Polyamides. Following a previously reported procedure,⁷ to a slurry of NaH (80 mg, 60% in mineral oil) in 0.5 mL DMF was added ethanethiol (0.32 mL), and the mixture was heated to 80 °C for 5 min. The polyamide (0.4 μmol) was

dissolved in DMF (0.25 mL), added to the ethanethiolate solution and the mixture was heated to 80 °C for 30 min in a sealed tube under periodic agitation. After cooling to 0 °C, glacial acetic acid (3 mL) was added and all volatiles removed in vacuo. The residue was dissolved in CH₃CN (0.5 mL) and 0.1% TFA (2 mL) and purified by preparative reversed-phase HPLC to yield the pure polyamides.

ImPyHzPy-(R)^H2^Nγ-PyPyPyPy-CONHMe (3). The title compound was recovered upon lyophilization of the appropriate fractions as a yellow powder (0.4 mg). UV (H₂O): λ_{max} 318, 254. MALDI-TOF-MS: calcd. for C₅₃H₅₈N₁₉O₉, 1105.1; found, 1105.1.

ImPyHpPy-(R)^H2^Nγ-PyPyPyPy-CONHMe (4). The title compound was recovered upon lyophilization of the appropriate fractions as a white powder (0.1 mg). UV (H₂O): λ_{max} 316, 244. MALDI-TOF-MS: calcd. for C₅₂H₆₀N₁₉O₁₀, 1111.1; found, 1111.7, 1133.7 (M+Na).

Construction of plasmid DNA. The plasmid pDR1 was constructed by hybridization of the two oligonucleotides 5'-GATCAGGCTGCTATGGACGGCTGCTGTGTATGGACG-GCTGCTGTTTATGGACG-GCTGCTGTATATGGACGG-CTGGGCGA-3' and 5'-AGCTTCGC-CCAGCCGTCATATACAGCAGCCGTCCTAAACAGCA-GCCGTCCATACACAGCAGCCGTCCATAGACAGCCT-3' followed by ligation into the *Bam*HI/*Hin*DIII restriction fragment of pUC19 using T4 DNA ligase. The resultant plasmid was then used to transform *E. Coli* XL-1 Blue Supercompetent cells. Ampicillin-resistant white colonies were selected from 25 mL Luria-Bertani agar plates containing 50 mg/mL ampicillin, treated with XGAL and IPTG solutions and grown overnight at 37 °C. Cells were harvested after overnight growth at 37 °C. Large-scale plasmid purification was performed with Qiagen purification kits. The presence of the desired insert was determined by dideoxy sequencing. DNA concentrations were determined at 260 nm using the relationship 1 OD unit = 50 μg/mL duplex DNA.

Preparation of 3'-End-Labeled DNA Restriction Fragments. The plasmid pDR1 was linearized with *Eco*RI and *Pvu*II and treated with the Klenow fragment of DNA polymerase II, [α-³²P]-dATP, and [α-³²P]-TTP for 3'-end labeling. The labeled 3'-fragment was purified on a 7% nondenaturing polyacrylamide gel (5% cross-linkage) and the desired 284 base pair band isolated after visualization by autoradiography. The DNA was precipitated with 2-propanol, the pellet washed, lyophilized, and resuspended in RNase-free H₂O. Chemical sequencing reactions were performed according to published protocols.²¹

DNase I Footprinting. All reactions were carried out in a volume of 400 μL according to published procedures. Quantitation by storage phosphor autoradiography and determination of equilibrium association constants were as previously described.¹⁹

Acknowledgment. We are grateful to the National Institute of Health (GM27681) for research support and the Swiss National Science Foundation for a postdoctoral fellowship to D.R. We thank M. A. Marques for guidance with the ab initio calculations.

Supporting Information Available: Ab initio calculations for four-ring polyamide subunits PyImPyIm and PyIpPyIm, PyHpPyIm and PyHzPyIm, and PyPyPyIm and PyBiPyIm (Figures S1, S2, S3). This material is available free of charge via the Internet at <http://pubs.acs.org>.

JA0300158